Journal of Applied Polymer Science

Low temperature cure of epoxy thermosets attaining high T_g using a uniform microwave field

Robert L. Hubbard,[1] S. Michael Strain,[2] Connor Willemsen,[3] David R. Tyler[3]

[1]Lambda Technologies, Inc, Morrisville 27560, North Carolina

[2]CAMCOR NMR Spectroscopy Facility, University of Oregon, Eugene Oregon 97403

[3]Department of Chemistry and Biochemistry, University of Oregon, Eugene Oregon 97403

Correspondence to: D. R. Tyler (E-mail: dtyler@uoregon.edu)

ABSTRACT: It is demonstrated for the first time that an epoxy thermoset resin can be cured at temperatures well below its $T_{g\infty}$. This study compared the use of a uniform variable frequency microwave (VFM) field to standard oven curing at temperatures above and below $T_{g\infty}$. Using T_g, tanδ, modulus, and FTIR measurements, it is shown that the reaction of BFDGE with MDA to attain a product with $T_{g\infty}$ of 133 °C is achieved by VFM at temperatures from 100 to 140 °C; in contrast, the thermal cure normally requires 170 °C to attain the same $T_{g\infty}$ and the same extent of cure. By following the pregel cure reaction with ^{13}C-NMR spectroscopy, it was determined that the lower cure temperatures of VFM cure predominately lead to chain extension and smaller amounts of crosslinking compared to the thermal cure. To explain these results, it is suggested that, after gelation, with VFM cure there is higher mobility from dipole rotations that continues the cure to completion without vitrification. © 2016 Wiley Periodicals, Inc. J. Appl. Polym. Sci. **2016**, *133*, 44222.

KEYWORDS: crosslinking; glass transition; manufacturing; resins; thermosets

Received 11 April 2016; accepted 17 July 2016

DOI: 10.1002/app.44222

INTRODUCTION

Epoxy composites for the consumer electronics industry are a growing 3.4 billion dollar a year market.[1] Device packaging, display assembly, case parts, circuit boards for smartphones, tablets, laptops, and game consoles all involve epoxy composites. The use of epoxies in the consumer electronics industry is challenging. As consumer products get smarter and smaller, epoxies are being required to join organic and inorganic materials with widely different modulus properties. In addition, multiple thermal excursions during assembly pose such difficult challenges that the assembly of electronic devices now accounts for a significant portion of the total costs of consumer electronics.[2]

Epoxy formulations have become quite complex, but the basic thermal behavior remains the same. The ultimate glass transition temperature ($T_{g\infty}$) needs to be high enough so that the epoxy does not soften and allow bonded joints and assembled parts to move even fractions of a millimeter with respect to each other. Hence, curing temperatures must be high. However, low curing temperatures are being sought to allow the use of low temperature plastics, which save cost, weight, and space in consumer products. Another issue is the direct relationship between epoxy cure temperature and stress. Shrinkage stress increases as the epoxy reaction product cools from the highest cure temperature in the gel state to ambient temperature.[3] As larger complex silicon devices are incorporated into common consumer products, thermal stress issues become more costly to alleviate.

It is well established that the thermal cure of thermosets, and in particular epoxies, requires a cure temperature above the ultimate glass transition temperature ($T_{g\infty}$) to achieve full cure without vitrification.[4–6] In a vitrified (glassy) state, the reaction becomes controlled by diffusion of the reactants and consequently is slowed by orders of magnitude. If vitrification occurs, chemical control of the reaction may be reestablished by heating to 10–15 °C above $T_{g\infty}$. In practice, with commercial epoxy adhesives, the actual cure temperatures are usually set to 50 °C higher than $T_{g\infty}$ to decrease the time of the cure process to 2 h.

After gelation, thermoset backbones become rigid, with crosslinking restricted to side-chain reactions. To continue the cure reaction requires increasing the temperature to increase mobility. One suggestion has been to reduce that cure time with microwave energy. The opportunity offered by microwave

Additional Supporting Information may be found in the online version of this article.

curing of polymers is the inherently different heating mechanism. In contrast to conventional heating, which creates molecular translational energy, microwave fields excite polarizable electrons in molecules, which creates rotational motion from dielectric loss (ε″).[7] This rotational energy provides increased collision frequencies and more favorable alignment of the reactive species, factors that directly increase reaction rates according to the collision-modified Arrhenius equation. Microwave excited rotations occur not only on the side chains but also along the backbones of polymers, greatly enhancing the mobility of the entire polymer network.[8] By this means, microwave fields increase the mobility of the "infinite network" formed at gelation so the cure can continue in the gel state at a lower temperature of the bulk material. However, highly varied results have been reported when microwave energy is used to increase the cure rate of epoxy resins.[9–11] For example, both low reaction rates and very high reaction rates have been reported with accompanying speculations of reaction mechanisms and structural dependencies. Furthermore, the common use of a single frequency microwave generator requires that a single mode, in a very small area (less than 1 cm^3) be the focus of the experiment. As a result of this difficult experimental condition, it is not surprising that "hot spots" of activation and cure, represented by broad glass transitions in the product DSC traces, were found.

With the development more than two decades ago of variable frequency microwave (VFM) technology,[12] it became possible to produce a highly uniform field over a volume of about 1 m^3 (a million-fold increase) from a single generator and waveguide. Consequently, sample temperature variations of only ±1.7 °C have been measured across large cavity chambers from wall to wall in all dimensions. Our VFM microwave oven changes frequencies every 25 μs. This technology eliminates the possibility of metal arcing found in single frequency systems. With these uniform VFM fields, it has been reported that polymerization of epoxy thermosets,[13–15] thermoplastic films,[16] and other polymer systems[17–20] have been cured at temperatures well below the standard thermal cure, with high extent of cure. In addition, there is evidence of modified thermomechanical properties in these systems, including modulus,[21] crosslink density, stress, and coefficient of thermal expansion.[22] Finally, it is noted that a low temperature epoxy cure resulting in a high $T_{g\infty}$ has been reported to produce lowered stress and increased reliability of an IBM microprocessor server module.[23] As a result of these benefits, VFM technology has been incorporated into production manufacturing systems world-wide.

In this study, we examine more closely the effects that microwave energy has on thermoset morphology and reaction pathways. The fundamental effect reported here is the capability of microwaves to avoid vitrification of epoxies at low cure temperatures. In consequence, the product epoxy has a high extent of cure and a high $T_{g\infty}$. This result is in contrast to the results obtained with standard convection oven curing.

EXPERIMENTAL

Previous studies of the thermal and microwave curing of epoxy resins used one of the commonly used bisphenol ethers (A or F) and a variety of curing agents, most often diaminodiphenyl sulfone (DDS) or methylene dianiline (MDA). Lange *et al.*[6] made a particularly thorough study of the thermal vitrification and gelation processes of the reaction of BFDGE and MDA (Figure 1) at temperatures above and below $T_{g\infty}$, so the reaction of these two compounds was the oven cure standard that we compared to microwave cure.

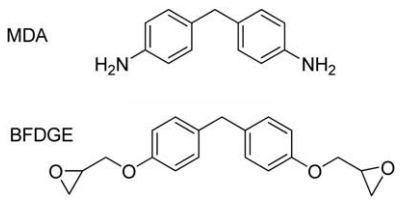

Figure 1. Structures of the starting material epoxide (BFDGE) and diamine (MDA) used in this study.

Materials

The reaction of bisphenol F diglycidylether (BFDGE; obtained as Epon 862 from Hexion Inc.) and methylene dianiline (MDA) (Aldrich) was investigated. The Epon 862 included approximately 20% of its dimer alcohol,[24] as determined by quantitative ^{13}C-NMR. The Epon 862 was used as received because the reference data used for oven cure comparison did not have the dimer removed.[6]

Methods

The BFDGE and MDA were mixed in a 2:1 stoichiometric ratio in all reactions because the BFDGE is difunctional and the MDA is tetra-functional. The waxy MDA and fluid BFDGE were thoroughly blended with mortar and pestle to make a slightly amber, non-viscous resin that was degassed for 30 min before use or until no further sign of outgassing could be seen.

The oven used for the thermal cure reactions was a ThermoScientific with a digital readout. A separate thermocouple in the oven chamber was used for confirmation. The VFM curing was performed in a Microcure 2100 model from Lambda Technologies with digital closed loop control based on the continuously measured temperature of the sample. A non-contact infrared probe provided temperature control of ±1 °C after emissivity calibration with a GaAs fiber optic probe directly in contact with the sample at each soak temperature. Power (maximum 500 W auto-leveled) was digitally controlled to produce ramp rates to soak with a precision of +/−2 °C. Typical power levels necessary for the samples ranged from a few watts during ramp to several hundred, depending on the soak temperature. Reflected power from the reaction chamber (13″ × 14″ × 15″) was found to always be less than 15%. Temperature variation within the microwave cavity had previously been measured to be ±1.7 °C. The programmed temperature profiles ended at the conclusion of the soak temperature time, and the samples passively returned to ambient temperature within 2–3 min because the air, fixtures, and walls of the chamber were not heated during microwave irradiation of the sample.

Samples for both oven and microwave cure were the same 42.5 × 8 × 1 mm^3 to facilitate measurement by DMA, with some of the length used to cut a sample for FTIR spectroscopy. Teflon molds

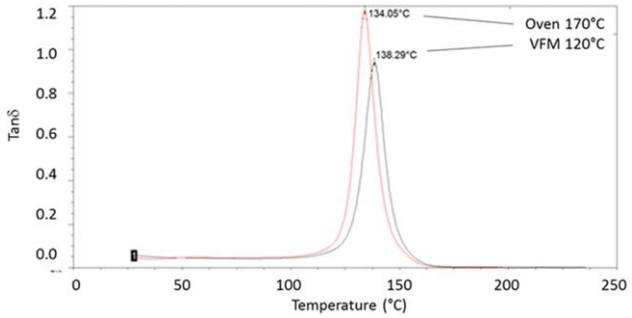

Figure 2. Overlay of the DMA measurements of tanδ maximum of samples cured in a standard oven at 170 °C and in a VFM oven at 120 °C (below the $T_{g\infty}$). [Color figure can be viewed in the online issue, which is available at wileyonlinelibrary.com.]

with cavities of these measurements were used for the curing experiments. The molds were cleaned and dried but not coated and the samples were easily removed with a spatula after cure. Teflon was used due to its microwave transparency and intermediate thermal conductivity. The molds were placed on Teflon rails in the center of the microwave chamber or on the center rack of the thermal oven.

DMA measurements[25] of ε′, ε″, and tanδ were made on a TA Instruments Q800 using a 3 °C/min ramp from 20 to 250 °C by single-cantilever vertical tension. Measurement of T_g was taken from the highest point of the tanδ peak and storage modulus was taken from a temperature 50 °C above the measured T_g.

FTIR measurements were taken on a diamond ATR adapter in a ThermoFisher 2000 spectrophotometer. The spectra were adjusted for ATR compensation and peak heights measured at 1269 cm^{-1} for loss of the primary amine peak from the MDA and at 1610 cm^{-1} for an unchanging phenyl peak from the MDA. The ratio of the 1269–1610 cm^{-1} peaks was chosen to monitor the progress of the condensation reaction because the loss of primary amine was a more direct measure than the opening of the epoxide ring because epoxide dimers in the starting material are known to be involved in the complex basic reaction autocatalysis.[3] As mentioned above, a substantial amount of dimer is included in the Epon 862 starting material.

^{13}C-NMR and ^{1}H-NMR measurements were taken on a Bruker Avance III-HD 600MHz spectrometer equipped with a Prodigy BBO multinculear cryoprobe and TopSpin 3.2pl6 software. Samples were dissolved immediately after curing in $CDCl_3$ (spectral grade) in a 5-mm precision NMR tube and run at 25 °C. "Quantitative" ^{13}C spectra were obtained with the following acquisition parameters: pulse sequence = zgig (^{1}H composite pulse decoupling (waltz-16) enabled only during acquisition to minimize NOE development; acquisition time aq = 1.0 s; relaxation delay d1 = 21 s; spectral width sw = 36,058 Hz; time domain size td = 72,110 points; pulse width, p1 = 10 us (90-deg flip); digitizer mode dm = baseopt; number of scans ns = 3000). Spectra were processed with apodization lb = 1.00; zero-filling si = 131,072 points; digital resolution 0.275 Hz/point; baseline correction = absn; peak area ratios were calculated from amplitude and linewidth values obtained with the TopSpin Lorentzian deconvolution (dcon) routine. ^{1}H/^{13}C-HMBC spectra were obtained with the TopSpin "hmbcgplpndqf" pulse sequence with 128 FID's in the f2 (^{1}H) dimension. The resulting digital resolution of the processed 2D spectrum was 2.5 Hz and 19.3 Hz in the f2 and f1 dimensions, respectively.

RESULTS AND DISCUSSION

BFDGE and MDA were reacted in a VFM microwave oven under a variety of conditions to determine the effect of various parameters on $T_{g\infty}$ of the resulting thermoset epoxy. The properties of the samples prepared by VFM were compared to the properties of materials prepared from the same starting materials cured in a conventional thermal oven. In addition to $T_{g\infty}$, the emphasis was on comparing the extents of cure in the two sets of products. It is well established that when the cure temperature is less than $T_{g\infty}$, an incomplete cure occurs as a result of vitrification of the gel. Vitrification was determined by FTIR, T_g, storage modulus, and tanδ measurements. In our experiments, the $T_{g\infty}$ for a BFDGE and MDA resin mixture averaged 133 °C for samples cured at 170 °C in a standard thermal oven for 30 min. This value, obtained from the tanδ maximum using tension-DMA, was somewhat lower than the 150 °C value reported by Lange *et al.*[6] for the same materials cured at the same time and temperature but measured by modulated DSC. However, the difference in $T_{g\infty}$ values is typical between these measurement techniques. A comparison of the maximum tanδ T_g measurements is shown in Figure 2. Note there is no significant change in the storage modulus (ε′) of the cured epoxy as the VFM cure temperatures decreases (Table I). The modulus measurements were made in the rubbery state at 50 °C above the T_g where calculations of crosslink density are usually made.

A typical VFM cure profile, shown in Figure 3, depicts the controlled ramp from ambient to soak temperature and the programmed hold at soak temperature for the set time. There is a frequency sweep of 4096 pulses from 5.85 to 7.0 GHz every 0.1 s. The profile ends with natural cooling back to ambient temperature, which is not shown.

DMA Results

As shown in Figure 4, the average T_g values for VFM cures at 140 and 120 °C rise only slightly with time to $T_{g\infty}$. The slight rise is consistent with very little initial vitrification. The samples cured at 100 °C show a more significant rise with soak time, which indicates the removal of vitrification and continued cure. Within a reasonable soak time, complete extent of cure results in a high $T_{g\infty}$. In contrast to these results, the VFM cure at

Table I. Elastic Modulus Comparisons for the Reaction of BFDGE and MDA

	Cure temp (°C)	E′ (MPa)
Oven	170	16.3
VFM	140	18.8
VFM	120	17.1
VFM	100	15.8
VFM	80	15.4

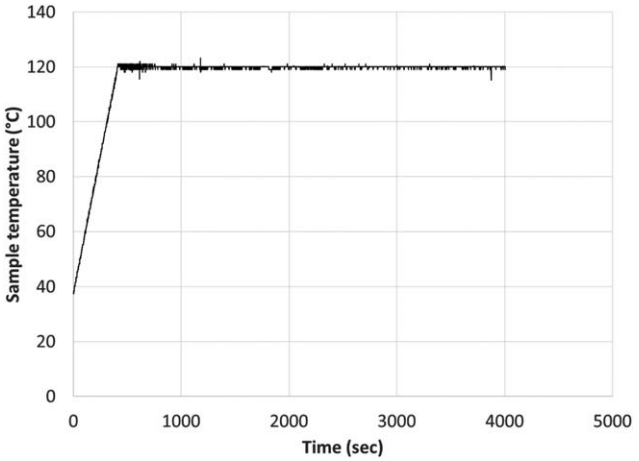

Figure 3. Sample VFM profile for the reaction of BFDGE and MDA. The ramp rate was 0.2 °C/s. The hold at 120 °C was for 60 min.

80 °C only shows a small increase with time, which indicates substantial vitrification even at long soak times.

Another measure of the transition from gel state to glassy state (vitrification) is the increase in tanδ with decreasing oven cure temperatures. As shown in Figure 5, only the 80 °C VFM cure shows a higher value in damping factor (tanδ) than that for the conventional cure at 170 °C.

FTIR Spectroscopy

The FTIR data for the oven-cured and VFM-cured reaction of BFDGE and MDA is shown in Figure 6. The ratio of the primary diamine MDA starting material absorbance to an unchanging phenyl absorbance decreases as the reaction progresses. The maximum loss is achieved quickly at 165 °C with oven cure and with VFM at 140 °C. The loss is slower at 120, 100, and 80 °C with VFM but still reaches the same level over longer time. These results are taken as direct evidence that VFM leads to a high extent of cure at low temperatures.

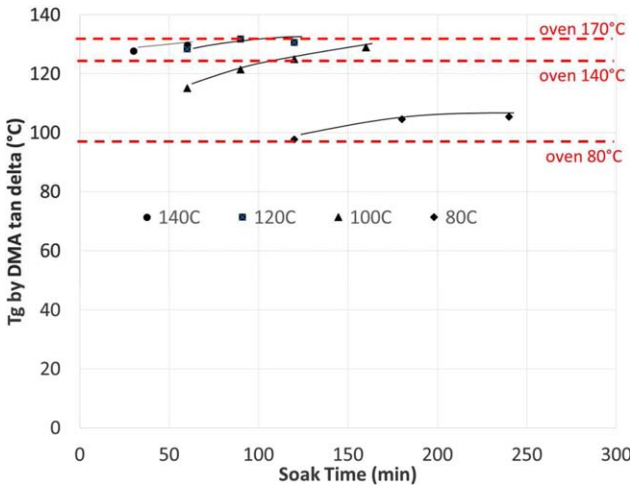

Figure 4. Measurement of extent of VFM cure by T_g vs. soak time at various temperatures. [Color figure can be viewed in the online issue, which is available at wileyonlinelibrary.com.]

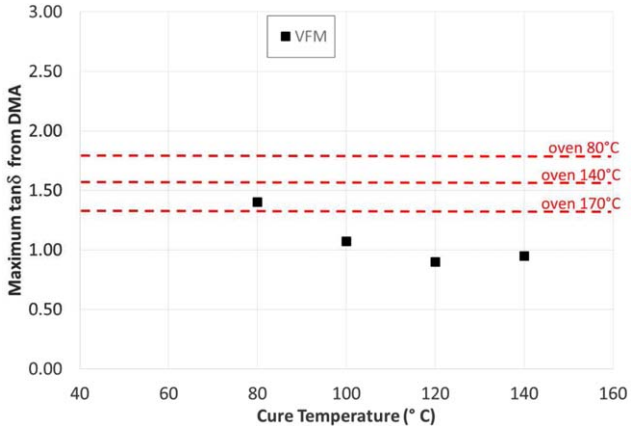

Figure 5. Comparison of the extent of vitrification of VFM cure to oven cure as measured by the value of tanδ. [Color figure can be viewed in the online issue, which is available at wileyonlinelibrary.com.]

Statistically Designed Experiments

With VFM it is possible to precisely control the ramp rate, soak temperature, and soak time variables. Consequently, two statistically designed experiments (DOE) with the three variables of temperature, time, and ramp rate were carried out. The initial data was fit to a non-orthogonal DOE over wide variable ranges (Supporting Information Tables S1–S3), which revealed a moderate interaction between temperature and time for T_g and the tanδ peak magnitude responses. There were no significant effects on modulus (ε′), nor were there any significant effects of ramp rate on any of the responses. A lack of effect of these variables on the storage modulus is consistent with the data in Table I.

With a temperature range limited to 80–140 °C, a new set of samples was designed into an orthogonal DOE matrix with center points (Supporting Information Tables S4–S6). The results for T_g (Figure 7) and tanδ (Figure 8) were similar to the first DOE (Supporting Information Tables S1–S3) but with a less significant interaction between temperature and time. The ramp rate was insignificant for any response. Temperature was about 25% stronger than time over this range. After about 90 min, both T_g and tanδ become the same as the samples cured in an

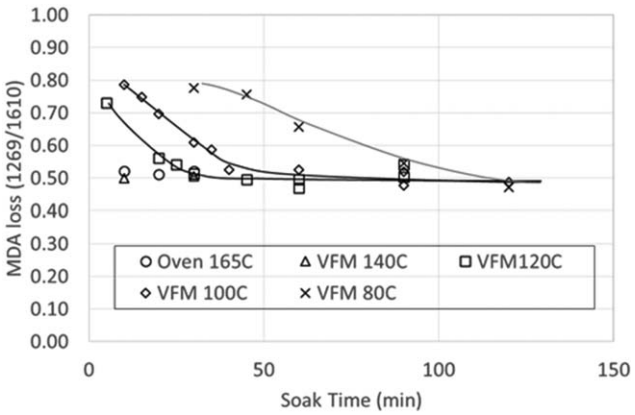

Figure 6. FTIR comparison of oven and VFM curing by the loss of the MDA starting material.

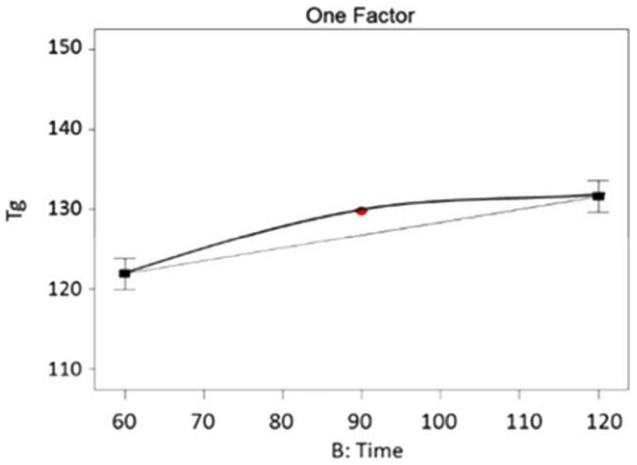

Figure 7. The increase of T_g with cure time at 100 °C with the statistical curvature shown in red. [Color figure can be viewed in the online issue, which is available at wileyonlinelibrary.com.]

oven above $T_{g\infty}$. The conclusion from these DOE experiments is that temperature is the primary method of preventing vitrification with VFM. Importantly, the effect of soak time is relatively insignificant after an initial period (after 90 min under these conditions). In industry, a typical cure time for this type of epoxy adhesive is 2 h to complete cure.

Investigation of the Pregelation Stage of the Reaction

In an attempt to monitor the progress of the reaction in the pregelation stage, during which the kinetics are chemically controlled, quantitative ^{13}C-NMR spectroscopy[26] was used to follow the amine concentrations. (Note that FTIR would not be useful because there is no tertiary amine absorbance to measure.) In Figure 9, the initial reaction of BFDGE (II) and MDA (I) is shown to form the first adduct (III), which is a secondary amine. At this point in the reaction (with a 2:1 stoichiometric ratio of epoxide to diamine), two possible products (IV) and (V) can form next, as shown in Figure 10.

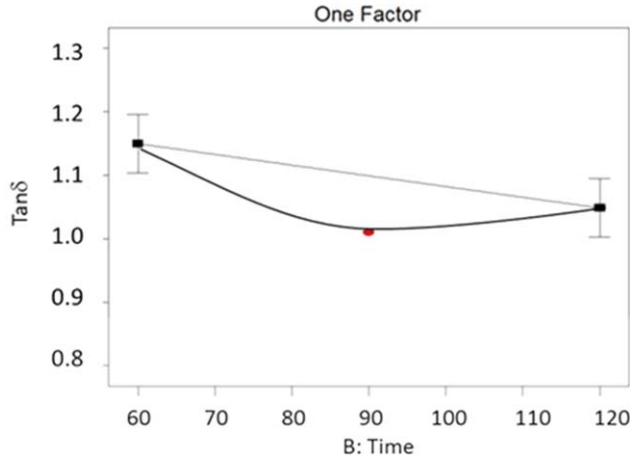

Figure 8. The decrease of tanδ with time at 100 °C with the statistical curvature shown in red. [Color figure can be viewed in the online issue, which is available at wileyonlinelibrary.com.]

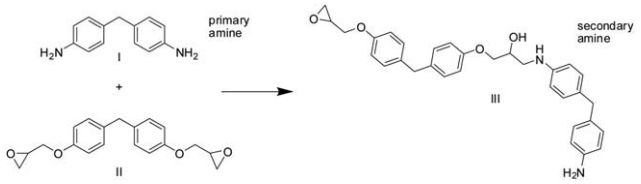

Figure 9. Initial reaction of MDA (I) and BFDGE (II).

It has been reported that the kinetics for the conventional oven cure of this second reaction (not in a solvent) is the same for either the secondary or tertiary amine.[27] In a solvent, there is a higher rate constant for the reaction with the secondary amine than the tertiary amine (1.5:1).[28] Fortunately, the ^{13}C-NMR spectrum of the reaction mixture before gelation (Figure 11) reveals clear separation of the carbons attached to the primary (MDA), secondary, and tertiary amine products. The positive identification of the peaks was confirmed by using the two-dimensional heteronuclear (H,C) HMQC data acquisition coupling technique. Peak area quantitation for the primary and secondary peaks were clearly defined, but for the closely spaced tertiary peaks ($T_1 = 7$ s), Lorentzian peak area fitting was necessary and successful. (For the very first minute or two of the reaction, the signal to noise of the growing tertiary peaks was too low for quantitation.)

As the reaction continues, substitution on the secondary amines of (IV) produce tertiary amine structures and, therefore, higher levels of crosslinking. These multiple, but not exactly identical, tertiary amines have slightly different ^{13}C chemical shifts around 131 ppm (Figure 11). In Figure 12, the ratio of the peak areas of each type of amine is plotted against the total amine peak area from the point at which the areas of the tertiary amine peaks become quantitative until gelation prohibits solubility in

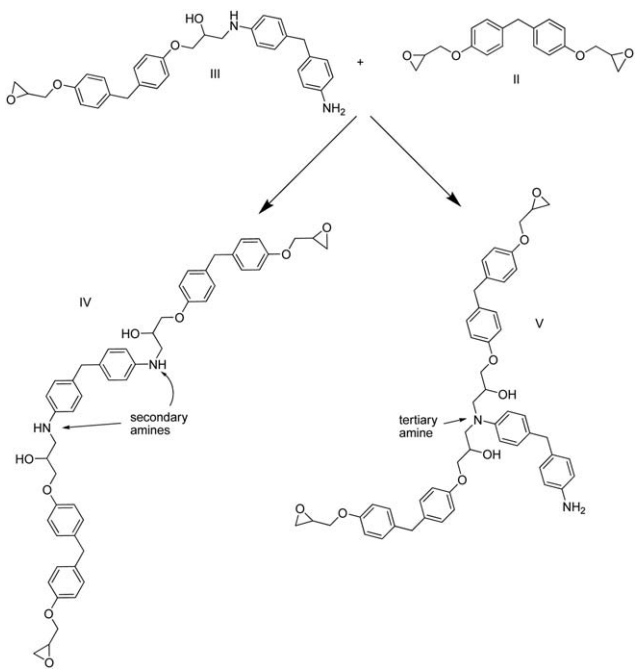

Figure 10. Addition of a second epoxide to (III) to form both linear (IV) and crosslinked (V) reaction paths.

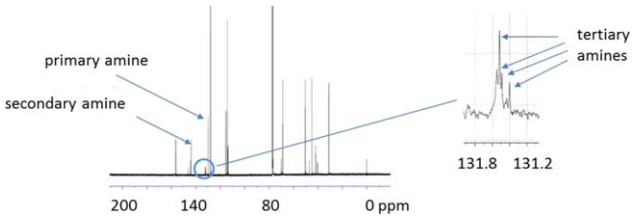

Figure 11. The ^{13}C NMR spectrum of the reaction between BFDGE and MDA before gelation. [Color figure can be viewed in the online issue, which is available at wileyonlinelibrary.com.]

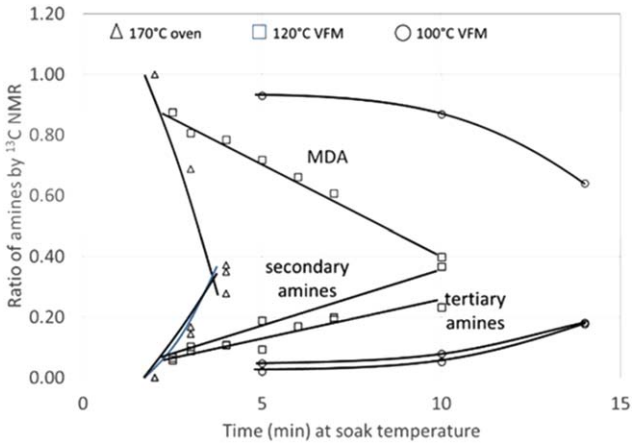

Figure 12. Peak area plots for the oven- and VFM-cured reaction of BFDGE and MDA at a selection of temperatures during the pregelation stage. [Color figure can be viewed in the online issue, which is available at wileyonlinelibrary.com.]

the $CDCl_3$ NMR solvent. Each data plot ends at the point of gelation. Notice in Figure 12 that the high temperature (165 °C) oven cure reaction (triangles) achieves gelation much sooner than the low temperature VFM cure reactions at 120 °C (squares) and 100 °C (circles). The tertiary amine data (black) in Figure 12 includes the sum of all the individual tertiary amine peak areas. As discussed next, additional information is

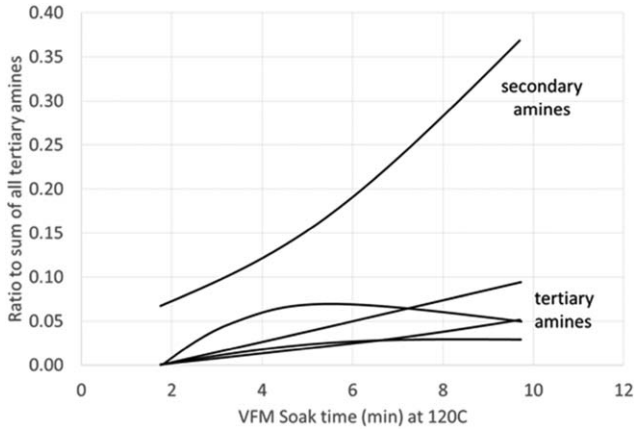

Figure 14. Relative amounts of secondary and tertiary amines before gelation for VFM cure at 120 °C.

obtained by separating the amounts of individual tertiary amines.

The relative amount of tertiary amine V (the first of the tertiary amines to be formed) would be expected to decrease as the amount of other tertiary amines in more highly crosslinked structures increases. As shown in Figure 13 (oven cure, 165 °C), this does indeed appear to be the case in that one of the tertiary amines rises and falls. Also note in Figure 13 that two of the tertiary amines increase rapidly before gelation, indicating a rapid rise in crosslinking of the network. In contrast, for the VFM reaction at 120 °C (Figure 14), all of the tertiary amines have a much lower rate of increase. Thus, under these conditions, the lower temperature VFM cure reaction produces more linear chain additions and fewer crosslinks before gelation than does the high-temperature oven-cure reaction. This result is quite different from the one-to-one ratio between linear backbone growth and crosslinking found in oven-cured resin systems. After gelation, when the reaction is hindered by the low mobility of the backbone and functional groups, it is the inherent nature of microwave dipole rotation to continue the cure reaction by creating more collisions of functional groups and by

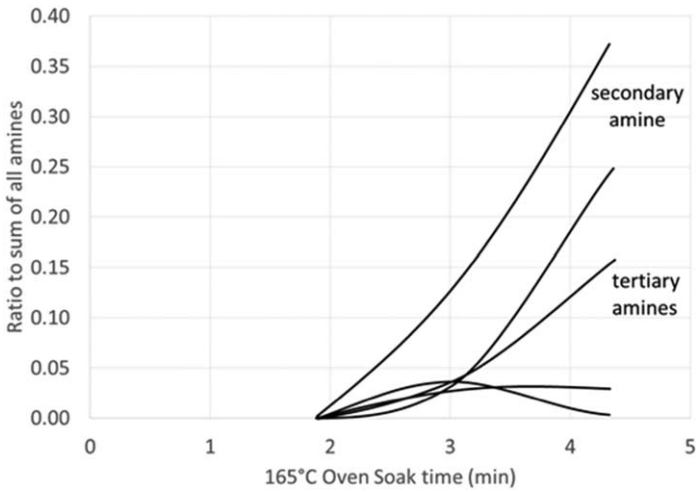

Figure 13. Relative amounts of secondary and tertiary amines before gelation for oven cure at 165 °C.

increasing the likelihood of favorable reactant orientation. Many positions along the backbone are also subject to rotation because there are many polarizable dipoles along the chain that are not involved in the reaction. All of this contributes to substantially higher reaction mobility well below the eventual $T_{g\infty}$.

CONCLUSIONS

Experimental results were presented that establish for the first time that an epoxy thermoset resin can be cured at temperatures well below the $T_{g\infty}$. This remarkable achievement is enabled by the use of a uniform VFM field. Earlier studies suggested that a microwave field is either ineffective[9,10] or too fast[11] to carry out an epoxy cure. The results presented above show that with a large and uniform multimode field such a cure can in fact be successful. This new capability allows the users of epoxy composites to obtain desirable high T_g values at low temperature cures. In industry, this technology provides thermal stability of adhesion joints and structural features with the advantage of using a low temperature cure process. Additional work is underway to further understand the microwave reaction mechanism in more detail and to determine how structural variations and reaction parameters in the epoxide reaction affect the cure.

ACKNOWLEDGMENTS

The authors thank Dan Foster and Professor Skip Rochefort at Oregon State University for the DMA-sample runs. Funding for shared instrumentation in the CAMCOR NMR Facility was provided by the American Recovery and Reinvestment Act of 2009 (National Science Foundation Award No. CHE-0923589) and the Oregon Nanoscience and Microtechnologies Institute (ONAMI).

REFERENCES

1. Electronics Adhesives Market, Adhesives Market Share, UV Curing Adhesives Industry Analysis, Electronic Components Market Size. Available at http://www.mordorintelligence.com/industry-reports/global-electronics-adhesives-market-industry (accessed Apr 7, **2016**).
2. Vardaman, J. *CEO of TechSearch International, personal communication.* **2016**.
3. Lee, H. L.; Neville, K. Handbook of Epoxy Resins; McGraw-Hill: New York, **1967**.
4. Prime, R. B. In Thermal Characterization of Polymeric Materials; Turi, E. A., Ed.; Academic Press: San Diego, **1997**.
5. Pascault, J. -P.; Sautereau, H.; Verdu, J.; Williams, R. J. J., Eds. Thermosetting Polymers; Marcel Dekker, Inc.: New York, **2002**.
6. Lange, J.; Altmann, N.; Kelly, C. T.; Halley, P. *J. Polym.* **2000**, *41*, 5949.
7. Metaxas, A. C.; Meredith, R. J. Industrial Microwave Heating, 1st ed.; Peter Peregrinus Ltd: London, UK, **1983**.
8. Rubinstein, M.; Colby, R. H. Polymer Physics, 1st ed.; Oxford University Press: Oxford, New York, **2003**.
9. Mijovic, J.; Wijaya, J. *Macromolecules* **1990**, *23*, 3671.
10. Mijovic, J.; Fishbain, A.; Wijaya, J. *Macromolecules* **1992**, *25*, 986.
11. Marand, E.; Baker, K. R.; Graybeal, J. D. *Macromolecules* **1992**, *25*, 2243.
12. Lauf, R.; Bible, D. W.; Johnson, A. C.; Everleigh, C. *Microwave J.* **1993**, 24.
13. Hubbard, R. L.; Zappella, P. *IEEE Trans. Compon. Packag. Manuf. Technol.* **2011**, *1*, 1957.
14. Tanaka, K.; Bidstrup Allen, S. A.; Kohl, P. A. *IEEE Trans. Compon. Packag. Technol.* **2007**, *30*, 472.
15. Diop, M. D.; Paquet, M. C.; Danovitch, D.; Drouin, D. *IEEE Trans. Device Mater. Reliab.* **2015**, *15*, 250.
16. Hubbard, R. L.; Garard, R. S. In *15th International Conference on Advanced Thermal Processing of Semiconductors RTP;* Catania, Italy, *2007*; pp 165–175.
17. Yota, J.; Ly, H.; Ramanathan, R.; Sun, H. C.; Barone, D.; Nguyen, T.; Katoh, K.; Ohe, M.; Hubbard, R. L.; Hicks, K. *IEEE Trans. Semicond. Manuf.* **2007**, *20*, 323.
18. Hubbard, R. L. *ECS Trans.* **2007**, *6*, 737.
19. Mead, P. F.; Ramamoorthy, A.; Pal, S. *J. Electron. Packag.* **2003**, *125*, 294.
20. Wang, T.; Liu, J. *J. Electron. Manuf.* **2000**, *10*, 181.
21. Hubbard, R. L. Effects of Underfill Curing on Substrate Warpage; IEEE: Phoenix, AZ, **2011**.
22. Hubbard, R. L.; Lee, B.-S. In International Wafer Level Packaging Conference; IWLPC: San Jose, CA, **2013**.
23. Diop, M. D.; Paquet, M. C.; Drouin, D.; Danovitch, D. In *IMAPS - International Microelectronics & Packaging Society;* Orlando, FL, **2013**; p 461.
24. Tanaka, Y.; Kakiuchi, H. *J. Appl. Polym. Sci.* **1963**, *7*, 1063.
25. Babayevsky, P. G.; Gillham, J. K. *J. Appl. Polym. Sci.* **1973**, *17*, 2067.
26. Sojka, S. A.; Moniz, W. B. *J. Appl. Polym. Sci.* **1976**, *20*, 1977.
27. Dusek, K. *Adv. Chem. Ser.* **1984**, *208*, 3.
28. King, J. J.; Bell, J. P. *ACS Symp. Ser.* **1979**, *114*, 225.